RSC Advances

ROYAL SOCIETY OF CHEMISTRY

www.rsc.org/advances

Design, synthesis and biological evaluation of a novel Cu^{2+}-selective fluorescence sensor for bio-detection and chelation

Yu Gao*, Yazhen Li, Xiping Yang, Fangfei He, Jiamei Huang, Minghong Jiang, Zaihui Zhou, Haijun Chen*

College of Chemistry, Fuzhou University, Fuzhou, Fujian, China, 350108

Corresponding authors:
*Yu Gao, PhD
College of Chemistry
Fuzhou University
Fuzhou, Fujian 350108, China
Email: hellogaoyu@126.com

*Haijun Chen, PhD
College of Chemistry
Fuzhou University
Fuzhou, Fujian 350108, China
Email: chenhaij@gmail.com

Abstract

A novel fluorescence sensor was designed and synthesized for detecting Cu^{2+} with high sensitivity and selectivity. The sensor showed a large red-shift in UV-vis spectra and obvious decline of fluorescent intensity in fluorescence emission spectra upon the addition of Cu^{2+}. The bio-imaging studies and flow cytometric analysis revealed that this sensor was cell-permeable and could be used for detection of the changes of intracellular Cu^{2+}, suggesting the suitability of this sensor for biological application. Cell cytotoxicity studies demonstrated it was capable of chelating excess Cu^{2+} *in vitro* to modulate the biological functions of Cu^{2+} with low cytotoxicity. Therefore, this compound could be one of the promising fluorescent sensors combining the abilities of either detection or modulation of the biological function of Cu^{2+} in biological conditions.

Keywords: Fluorescent sensor, Cu^{2+}-selective, bio-imaging, bio-detection, chelation.

1 Introduction

Copper plays an important role in biology and living organisms. As an essential transition element, copper could exert regulatory or catalytic activity in structurally-constrained binding sites in metalloproteins in cells. Dietary copper in the Cu^{2+} state is absorbed from the small intestine and enter the portal circulation to reach the liver. The copper in the hepatocytes is distributed to the whole body wherever needed and the excess of copper is excreted from the hepatic cells into the bile and discharged with the feces.[1] The disorders of the uptake, storage, trafficking and excretion of Cu^{2+} may lead to a variety of diseases including Menkes disease,[2] Wilson's disease,[3] and Alzheimer's disease (AD).[4] In addition, as a redox-active metal, copper may promote formation of toxic hydroxyl radicals and induce protein mis-folding and aggregation. Exposure to high levels of Cu^{2+} could cause liver and kidney damage.[5] Therefore, the Cu^{2+} concentration should be tightly confined to keep its homeostasis. The average concentration of blood copper is 15.7-23.6 μM.[6]

In this connection, considerable efforts have been made in developing specific chemosensors for monitoring Cu^{2+} in vitro and in vivo. Detection and quantification of Cu^{2+} by specific sensors is important for understanding the pathological role of copper in nature. A variety of methods have been developed for diagnosis of copper in biological conditions.[7, 8] Among them, fluorescent probes are regarded as the most preferable approaches for measurement copper with high selectivety, sensitivity, and simplicity. A number of fluorescent sensors based on different fluorophores such as coumarin,[6] BODIPY,[9] fluorescein,[10] naphthalimide,[11] and others[12] were developed to detect Cu^{2+} in biological conditions.

Besides detection of Cu^{2+}, increasing attention has been paid to the elimination or chelation of excess Cu^{2+} from the organisms. Chelation therapy is proved to be of crucial important in the

long-term treatment of metal storage diseases.[13] Trientine, D-penicillamine, and meso-2,3-dimercaptosuccinic acid were efficient antidotes used in clinical for treatment of Wilson's disease. As the personalized therapy becomes a trend of future medical development, great advances have been made in the field of theranostics which combines both diagnostics and therapeutics.[14, 15] Accordingly, some fluorescent nanoparticles have been designed for selective detection and simultaneously removal of Cu^{2+} to monitor and reduce the harm of Cu^{2+} in living systems.[16, 17] Although many fluorescent materials have the ability to detect Cu^{2+} in biological conditions by fluorescence changes, they scarcely have ability to chelate the excess Cu^{2+} at the same time.

Here, we designed and synthesized a new coumarin-based Cu^{2+}-selective fluorescent sensor (**FZU-06,001**) and investigated the potential application of this fluorescent sensor for detection and chelation of Cu^{2+} in cultured cells. This new compound may act as a theranostic agent to either imaging or removal of Cu^{2+}.

2. Experimental section

2.1 Materials and equipments

All reagents were commercially purchased, and the solvents were used after appropriate distillation or purification. Chloride and nitrate salts of Na^{+}, Ca^{2+}, Mg^{2+}, K^{+}, Ni^{2+}, Fe^{2+}, Co^{2+}, Hg^{2+}, Ag^{+}, Cu^{2+}, Cd^{2+} (Aldrich and Alfa Aesar) were used during experiment. HEPES buffer solutions (20 mM, pH 7.4) were prepared in water. Proton and carbon nuclear magnetic resonance (^{1}H and ^{13}C NMR) spectra were recorded on a Bruker Avance 400 spectrometer with tetramethylsilane (TMS) as an internal standard. Chemical shifts are reported as δ values (ppm) down-field from internal TMS of the indicated organic solution. Peak multiplicities are

expressed as follows: s, singlet; d, doublet; t, triplet; q, quartet and m, multiplet. Mass spectra were obtained using a Waters Micromass Q-Tof mass spectrometer. Purities of the compounds were established by analytical HPLC, which was carried out on a Shimadzu HPLC system (model CBM-20A LC-20AD SPD-20A UV/vis). HPLC analysis conditions were as follows: Inertstil ODS2 C18 (150 mm × 4.6 mm, 5 μm) column; flow rate, 0.5 mL/min; UV detection at 420 nm; linear gradient from 10% methanol in water to 100% methanol in water in 20 min followed by 10 min of the last-named solvent. UV-vis absorption spectra were carried out on a Shimadzu UV-2450 UV-VIS spectrophotometer. Fluorescence spectra were measured on Edinburgh FL900/FS900 spectrophotometer. The absolute fluorescence quantum yield (Φ_F) was measured with a Quantaurus-QY absolute photoluminescence quantum yield measurement system (Hamamatsu, C11347-11).[18] The cell viability was measured with a microplate reader (MULTISKAN MK3, Thermo SCIENTIFIC). The intracellular localization was observed by a Leica TCS SP8 confocal laser-scanning microscope (Leica, Germany). The intracellular Cu^{2+} detection experiments were imaged by an inverted fluorescence microscope (IX71, Olympus, Japan). The flow cytometry was carried out by a Coulter EPICS XL flow cytometer (Beckman Coulter Co. Ltd., FL, USA).

2.2 Synthesis

2.2.1 7-(Diethylamino)-2-oxo-N-(quinolin-8-yl)-2H-chromene-3-carboxamide (FZU-06,001)

To a solution of 7-(diethylamino)-2-oxo-2*H*-chromene-3-carboxylic acid [19] (**3**, 60 mg, 0.23 mmol) and 8-aminoquinoline (**4a**, 33 mg, 0.23 mmol) in 1 mL of dimethylformamide (DMF) was added 2-(1*H*-benzotriazol-1-yl)-1,1,3,3-tetramethyluronium hexafluorophosphate (HBTU) (104 mg, 0.28 mmol). *N*,*N*-diisopropylethylamine (DIPEA) (60 mg, 0.46 mmol) was added at 0

^{o}C. The resulting mixture was stirred at r.t. for 16 h. The reaction mixture was diluted with ethyl acetate (AcOEt) (100 mL) and washed with water (30 mL). The organic layer was separated and dried with anhydrous Na_2SO_4. The solution was concentrated to give a crude product, which was purified with silica gel column (CH_2Cl_2/MeOH = 10/1) to obtain the desired product (70 mg, 79%) as a yellow solid (mp 226-227 ^{o}C). HPLC purity 95.5% (t_R = 20.45 min). ^{1}H NMR (400 MHz, $CDCl_3$): δ 12.77 (s, 1H), 8.99-9.00 (m, 2H), 8.85 (s, 1H), 8.16 (d, 1H, *J* = 8.0 Hz), 7.53-7.59 (m, 2H), 7.45-7.49 (m, 2H), 6.67 (d, 1H, *J* = 8.0 Hz), 6.55 (s, 1H), 3.47 (q, 4H, *J* = 8.0 Hz), 1.26 (t, 6H, *J* = 8.0 Hz). ^{13}C NMR (100 MHz, DMSO-*d*$_6$): δ 161.7, 161.0, 157.6, 152.8, 149.1, 148.4, 138.5, 136.5, 135.1, 131.9, 127.9, 127.0, 122.1, 121.9, 116.8, 110.3, 109.2, 108.0, 95.9, 44.4, 12.3. HRMS (ESI) calcd for $C_{23}H_{22}N_3O_3$ 388.1656 $(M + H)^+$, found 388.1657.

2.2.2 7-(Diethylamino)-N-(naphthalen-1-yl)-2-oxo-2H-chromene-3-carboxamide (FZU-06,002)

FZU-06,002 was prepared in 85% yield by a procedure similar to that used to prepare **FZU-06,001**. The title compound was obtained as a yellow solid (mp 202-203 ^{o}C). HPLC purity 99.9% (t_R = 21.56 min). ^{1}H NMR (400 MHz, $CDCl_3$): δ 11.53 (s, 1H), 8.87 (s, 1H), 8.44 (d, 1H, *J* = 8.0 Hz), 8.22 (d, 1H, *J* = 8.0 Hz), 7.87 (d, 1H, *J* = 8.0 Hz), 7.67 (d, 1H, *J* = 8.0 Hz), 7.59 (t, 1H, *J* = 8.0 Hz), 7.49-7.54 (m, 3H), 6.69 (d, 1H, *J* = 8.0 Hz), 6.56 (s, 1H), 3.49 (q, 4H, *J* = 8.0 Hz), 1.27 (t, 6H, *J* = 8.0 Hz). ^{13}C NMR (100 MHz, DMSO-*d*$_6$): δ 162.9, 160.9, 157.4, 152.8, 148.4, 133.6, 133.2, 131.9, 128.7, 126.5, 126.1, 125.9, 125.3, 124.1, 120.3, 117.6, 110.5, 109.0, 108.0, 95.9, 44.4, 12.3. HRMS (ESI) calcd for $C_{24}H_{21}N_2O_3$ 385.1558 $(M - H)^-$, found 385.1558.

2.3 Absorption and fluorescence spectra

Inorganic salt was dissolved in distilled water to afford 20 mM aqueous solution. Stock solutions of **FZU-06,001** and **FZU-06,002** (2 mM) were prepared in absolute DMSO. All the measurements were carried out according to the following procedure. To 1.5 mL centrifuge tube containing 10 μL of the stock solution of **FZU-06,001** or **FZU-06,002**, 990 μL of metal ions (containing 10 μL 20 mM inorganic salt solution) diluted with HEPES buffer solution (pH 7.4, 20 mM) was added directly to the centrifuge tube. For the measurements of fluorescence spectra, excitation was set at 442 nm and emission was set over the range of 450-800 nm. The titration experiments were performed by mixing **FZU-06,001** with various concentrations of Cu^{2+} solution. The concentrations of Cu^{2+} solutions were varied, but the total volume was fixed at 1 mL and the total concentration of **FZU-06,001** was 20 μM. For the titration measurements of fluorescence spectra, excitation was set at 442 nm and emission was set over the range of 500-800 nm.

2.4 Cell culture

The cell lines Hela (Human epithelial carcinoma cell line) and HepG2 (Human hepatocellular liver carcinoma cell line) cells were obtained from the Cell Resource Center of Shanghai Institute for Biological Sciences (Chinese Academy of Sciences, Shanghai, China). Hela was grown in DMEM containing 10% fetal bovine serum (FBS), 100 U/mL penicillin G sodium and 100 μg/mL streptomycin sulfate. HepG2 was cultured in RPMI 1640 medium supplemented with 10% FBS and 1% antibiotics (100 U/mL penicillin G and 0.1 mg/mL streptomycin). Cells were maintained at 37 °C in a humidified and 5% CO_2 incubator.

2.5 MTT assay

Hela and HepG2 cells were cultured on 96-well plates at a density of 8,000 cells/well. The cells were incubated for 24 h to allow for attachment to the culture vessel before they were washed with prewarmed sterile PBS (pH 7.4), followed by exposition to **FZU-06,001** diluted with culture medium to various concentrations for 48 h at 37 °C. Then cell viability was evaluated by MTT assay. The amount of MTT formazan product was analyzed spectrophotometrically at 570 nm using a microplate reader. The cell viability (%) was calculated according to the following equation: Cell viability (%) = OD_{570}(sample)/OD_{570}(control) ×100. All drug concentrations were tested in six replicates.

2.6 Intracellular Localization

HepG2 cells were cultured on 10-mm^2 glass coverslips placed in 24-well plates and incubated for 24 h. Then the medium was replaced by fresh medium with 10 μM **FZU-06,001** and incubated for 2 h. The cells were rinsed with physiological saline, stained by Lysotracker Red DND-99 (from Molecular Probes, Eugene, OR) and Hoechst 33342 for 30 min, and fixed with 4% paraformaldehyde immediately. Subcellular localization was determined using confocal microscopy (Leica SP8 Microsystems Inc.). **FZU-06,001** was excited at 488 nm and monitored at 495-540 nm, LysoTracker Red was excited at 552 nm and monitored at 560-610 nm, and Hoechst 33342 was excited at 405 nm and monitored at 460-490 nm.

2.7 Intracellular Cu^{2+} detection

For intracellular Cu^{2+} detection by fluorescent imaging, Hela and HepG2 cell monolayers were cultured on 10 mm^2 glass coverslips for 24 h. After incubation with 10 μM **FZU-06,001** for 2 h at 37 °C, 10 equiv of Cu^{2+} were added into the culture media and cells were incubated for

further 0.5 h. Then cells were washed three times with PBS (pH 7.4) followed by visualized with a fluorescence microscope (Olympus-IX71) through green channel.

For intracellular Cu^{2+} detection by flow cytometry, Hela and HepG2 cells were seeded in a 24-well plate with 0.5 mL growth medium and allowed to attach for 24 h. Then, cells were incubated with 10 μM **FZU-06,001** for 2 h at 37 °C. After 0.5 h incubation with 10 equiv of Cu^{2+} solution, cells were washed three times with PBS (pH 7.4). Finally, cells were detached, subjected to flow cytometry. An excitation wavelength of 488nm was used with fluorescence emission measured at 530 ± 15 nm through fluorescence channel 1 (FL1).

2.8 Chelation efficacy

Hela and HepG2 cells were cultured on 96-well plates at a density of 8,000 cells/well. The cells were incubated for 24 h to allow for attachment to the culture vessel before they were washed with prewarmed sterile PBS (pH 7.4), followed by exposition to 5, 10, or 20 μM Cu^{2+} in the presence or absence of **FZU-06,001** at the same concentration for 24 h at 37 °C. Then cell viability was evaluated by MTT assay as described above. All drug concentrations were tested in six replicates.

2.9 Statistical analysis

Statistical analysis was performed using a Student's *t*-test. The differences were considered significant for $p < 0.05$ and $p < 0.01$ indicative of a very significant difference.

3. Resutls

3.1 Synthesis of FZU-06,001 and FZU-06,002

As shown in Scheme 1, compounds **FZU-06,001** and **FZU-06,002** were synthesized in 79% and 85% yields via a simple one-step procedure from the starting material 7-(diethylamino)-2-oxo-2*H*-chromene-3-carboxylic acid (**3**),[19] respectively. The moieties of 8-aminoquinoline and 1-aminonaphthalene were designed to compare the binding modes. The binding mode of **FZU-06,001** with Cu^{2+} is illustrated in Scheme 2. The structure of **FZU-06,001** and **FZU-06,002** were confirmed by ^{1}H-NMR, ^{13}C-NMR, and HRMS.

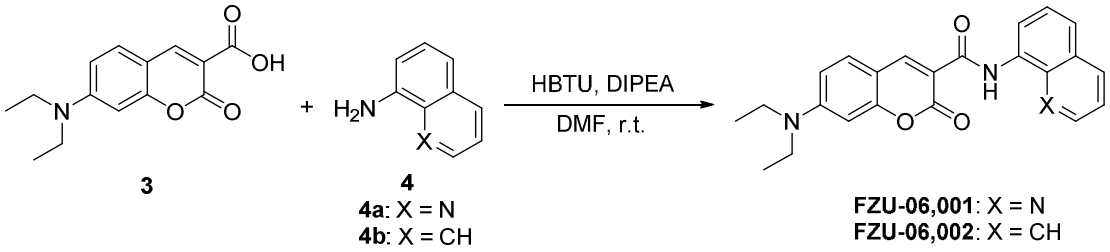

Scheme 1 Synthesis of **FZU-06,001** and **FZU-06,002**.

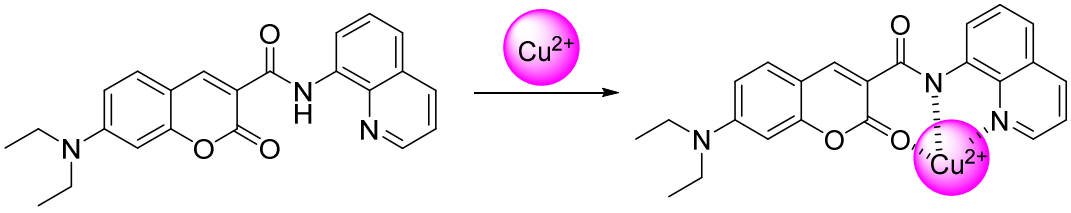

Scheme 2 Schematic illustration of the binding mode of **FZU-06,001** with Cu^{2+} ion.

3.2 Absorption and fluorescence studies with various metal ions

The selectivity of **FZU-06,001** and **FZU-06,002** to various metal ions was first examined under simulated physiological conditions with 20 mM HEPES buffer (pH 7.4). Fig. S1 shows the absorption spectra of **FZU-06,001** and **FZU-06,002** upon addition of different ions including Na^{+}, Ca^{2+}, Mg^{2+}, K^{+}, Ni^{2+}, Fe^{2+}, Co^{2+}, Hg^{2+}, Ag^{+}, Cu^{2+}, Cd^{2+}. Between 350 nm and 500 nm, the

UV-vis absorption of **FZU-06,001** and **FZU-06,002** exhibited a maxium absorption at 426 nm (log ε = 4.32 $M^{-1} \cdot cm^{-1}$) and 422 nm (log ε = 4.33 $M^{-1} \cdot cm^{-1}$), respectively. Addition of 10 equiv of Cu^{2+} resulted in red shift of **FZU-06,001** from 426 nm to 448 nm. No significant absorption maximum changes were found by mixing **FZU-06,001** with other inorganic salts. In contrast, no absorption changes were found of **FZU-06,002** responding to Cu^{2+} and other inorganic salts. The color changes of **FZU-06,001** (20 μM) and **FZU-06,002** (20 μM) with addition of chloride and nitrate salts could be observed by naked eyes. The color of **FZU-06,001** turned to deep yellow upon addition of 10 equiv of Cu^{2+} (Fig. S2). However, no obvious changes were found in other samples.

Fig. 1A and 1B showed the fluorescence spectra of **FZU-06,001** and **FZU-06,002** upon addition of different ions. The fluorescence spectra were obtained by excitation at 442 nm and emission over the range of 450–800 nm. Free **FZU-06,001** and **FZU-06,002** exhibited a strong fluorescence emission at 570 nm and 572 nm, respectively (Fig. S3). The 10 equiv of Cu^{2+} almost quenched the fluorescence of **FZU-06,001**, while no significant fluorescence changes were observed in **FZU-06,002**. Other ions tested had no obvious effects on the fluorescence changes of either **FZU-06,001** or **FZU-06,002**. The binding mode of **FZU-06,001** and Cu^{2+} is illustrated in Scheme 2. As expected, **FZU-06,001** with the moiety of aminoquinoline behaved as an additional binding site for the Cu^{2+} ion, while **FZU-06,002** bearing the unit of aminonaphthalene without nitrogen nearby did not have this function. The sensing selectivity of **FZU-06,001** towards Cu^{2+} was evaluated by adding 1 equiv of various metal ions including Ca^{2+}, Cd^{2+}, Fe^{2+}, K^{+}, Mg^{2+}, Na^{+}, Ag^{+}, Co^{2+}, Hg^{2+}, Ni^{2+}, respectively. As shown in Fig. 1C, the addition of other metal ions did not significantly alter the emission ratio (F458/F567) of **FZU-06,001**

except for the addition of Cu^{2+}. Moreover, the ratiometric sensing behavior of **FZU-06,001** to Cu^{2+} experienced no interference by the presence of other metal ions.

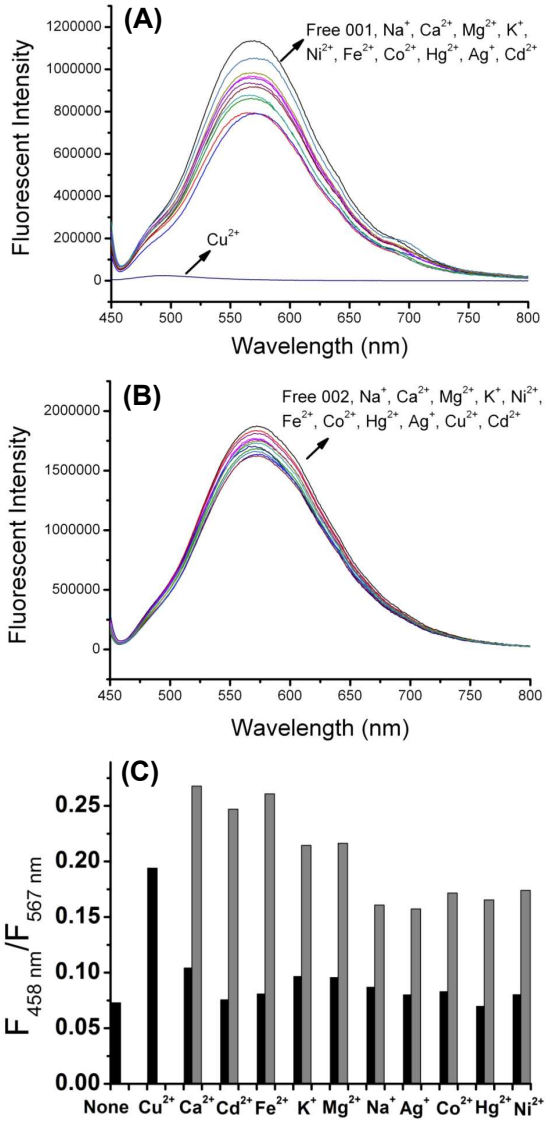

Fig. 1 Fluorescence spectra of **FZU-06,001** (20 μM) (A) or **FZU-06,002** (20 μM) (B) with addition of chloride and nitrate salts of Na^+, Ca^{2+}, Mg^{2+}, K^+, Ni^{2+}, Fe^{2+}, Co^{2+}, Hg^{2+}, Ag^+, Cu^{2+}, Cd^{2+} at concentration of 200 μM in HEPES buffer solutions (20 mM, pH 7.4) with the excitation at 442 nm. (C) Emission ratio at 458 and 567 nm (F458/F567) of **FZU-06,001** (20 μM) in HEPES buffer (20 mM, pH 7.4) induced by different metal cations. Black bars represent the F458/F567 ratio of free sensor or in the presence of 1 equiv of Cu^{2+}, Ca^{2+}, Cd^{2+}, Fe^{2+}, K^+, Mg^{2+}, Na^+, Ag^+, Co^{2+}, Hg^{2+}, Ni^{2+}. Grey bars represent the F458/F567 ratio of **FZU-06,001** determined after the addition of 1 equiv of indicated metal ions followed by addition of 1 equiv of Cu^{2+} with the excitation at 442 nm.

3.3 Absorption and fluorescence titration of FZU-06,001 with Cu^{2+}

Absorption and fluorescence titration of **FZU-06,001** with Cu^{2+} was performed to study detect limit of **FZU-06,001** to sense the Cu^{2+} concentration. Fig.2 shows the changes of absorption and fluorescence spectra of **FZU-06,001** upon addition of different concentrations of Cu^{2+} in HEPES solution. The absorption spectrum of **FZU-06,001** responds to the range of 0-20 μM of Cu^{2+} by measuring the absorbance of **FZU-06,001** solution from 300 nm to 650 nm. The absorbance decreased slowly at 426 nm and increased at 448 nm. The stoichiometry of **FZU-06,001** and Cu^{2+} was determined by the Job's method for absorbance measurement.[20] Maximum absorption intensity was observed when the molecular fraction of Cu^{2+} was 0.5, indicating 1:1 stoichiometric complex formation (Fig. 2A). The absolute fluorescence quantum yield (Φ_F) of **FZU-06,001** in aqueous solution (final concentration of **FZU-06,001** is 10 μM, H_2O:DMSO = 2000:1, v/v) is 0.04. The fluorescence change of **FZU-06,001** also responds to the range of 0-20 μM of Cu^{2+} (Fig. 2B). When excited at its excitation maximum of 442 nm, **FZU-06,001** showed one characteristic fluorescence band at 567 nm. The emission decreased linearly with Cu^{2+} concentration from 2 to 20 μM ($R^2 = 0.997$). The fluorescence was almost completely quenched when the ratio of **FZU-06,001** and Cu^{2+} reached 1:1. Using the fluorescence titration data, the binding constant of **FZU-06,001** with Cu^{2+} in aqueous solution was found to be $(9.14 \pm 1.43) \times 10^4$.[6, 20]

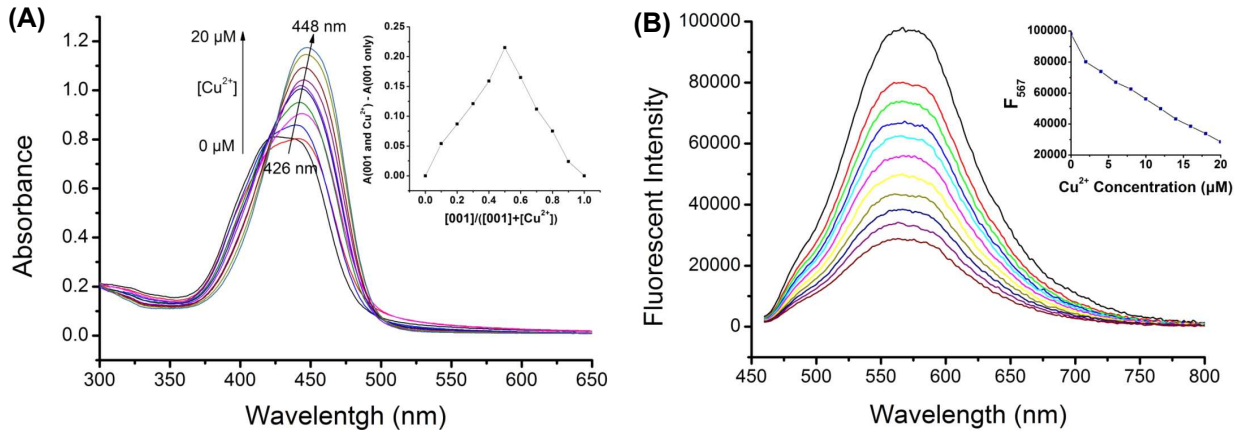

Fig. 2 (A) Absorbance spectra of **FZU-06,001** (20 μM) upon the titration of Cu^{2+} (0, 0.1, 0.2, 0.3, 0.4, 0.5, 0.6, 0.7, 0.8, 0.9, 1.0 equiv) in HEPES buffer solutions (20 mM, pH 7.4). The inset shows the Job's plot for **FZU-06,001** (20 μM) upon the titration of Cu^{2+}. (B) Fluorescence spectra of **FZU-06,001** (20 μM) upon the titration of Cu^{2+} (0, 0.1, 0.2, 0.3, 0.4, 0.5, 0.6, 0.7, 0.8, 0.9, 1.0 equiv) in HEPES buffer solutions (20 mM, pH 7.4) with the excitation at 442 nm.

3.4 Cytotoxicity of FZU-06,001

The cytotoxicity was first evaluated to determine the safe concentration of **FZU-06,001** for bio-application. MTT assays were conducted with Hela and HepG2 cells to test the cytotoxicity of **FZU-06,001**. As shown in Fig. 3, the cell viability remains more than 80% after treated with 20 μM **FZU-06,001** for 48 h. The results indicated that **FZU-06,001** is almost no cytotoxicity for long time incubation and suggested that **FZU-06,001** would be safe as a fluorescent imaging agent.

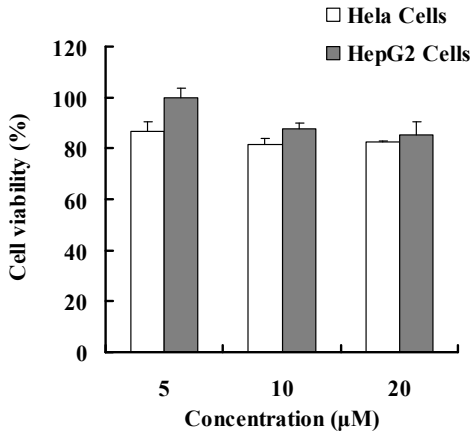

Fig. 3 Cytotoxicity of **FZU-06,001** in Hela and HepG2 cells. Hela and HepG2 cells were incubated with **FZU-06,001** at concentrations ranging from 5 to 20 μM for 48 h. Each data point represents the mean ± SD of six replicates.

3.5 Intracellular Localization

To investigate whether **FZU-06,001** could enter the cancer cells and which organelle it was apt to distribute, confocal laser scanning microscopy was used to observe the intracellular localization. The HepG2 cells were first incubated with **FZU-06,001** in the culture medium for 2 h and then stained with LysoTracker Red and Hoechst 33342, which are specific dyes for lysosome and nuclear, respectively. With 2 h incubation time, **FZU-06,001** could enter the HepG2 cells and distributed the whole cells (Fig. 4). The observed yellow fluorescence where the red and green of the image overlap revealed the distribution of **FZU-06,001** into the lysosomes. With Hoechst 33342 staining, some green fluorescence was co-localized in the blue area, indicating that **FZU-06,001** distributed in the nuclear.

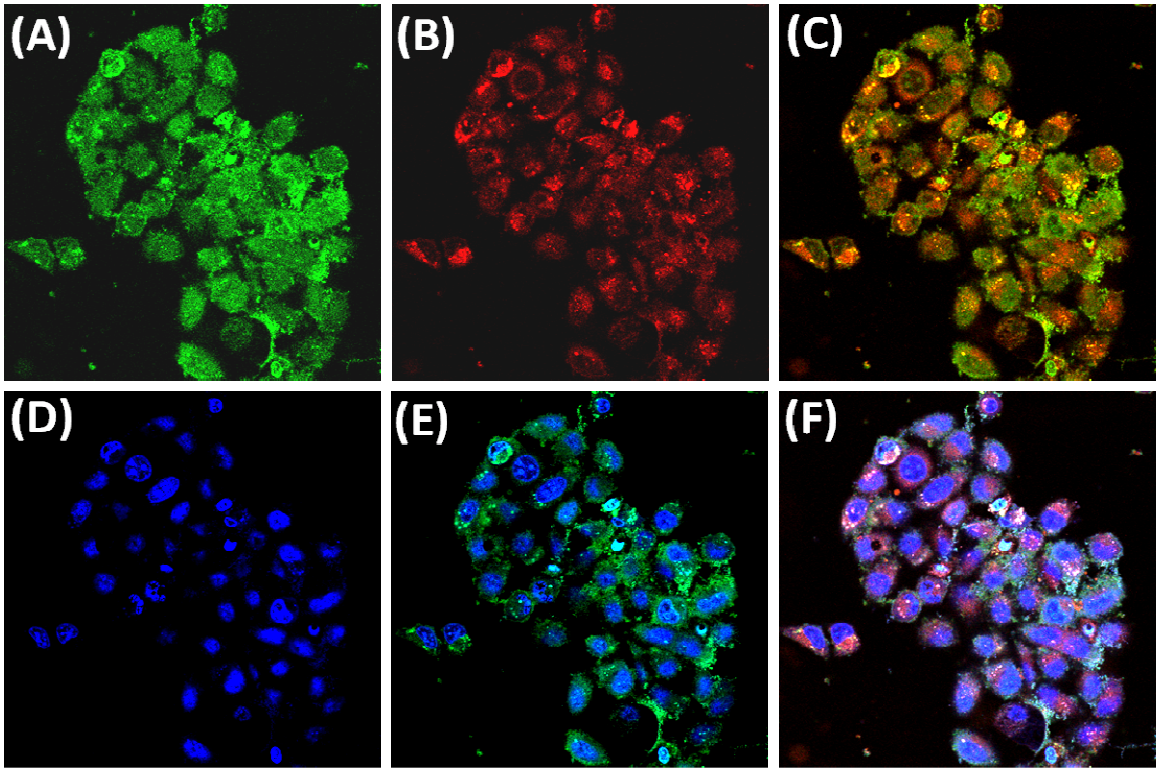

Fig. 4 Confocal images of HepG2 cells after treatment of **FZU-06,001** and after the fluorescence-labeling experiments. (A) Green fluorescence from **FZU-06,001**. (B) Red fluorescence from LysoTracker Red DND-99 for lysosomes. (C) Colocalization of red and green fluorescence observed in cells. (D) Blue fluorescence from Hoechst 33342 for nuclear. (E) Colocalization of blue and green fluorescence observed in cells. (F) Colocalization of triple fluorescence observed in cells.

3.6 Intracellular Cu^{2+} detection

The intracellular Cu^{2+} detection by **FZU-06,001** was also observed by fluorescent microscope. To avoid the influence of the sensor on cell function, the concentration of **FZU-06,001** was set at 10 μM which is safe enough for detection. **FZU-06,001** demonstrated good cell permeability. After 2 h incubation, the fluorescence could be seen in Hela and HepG2 cells by fluorescent microscope in the green channel (Fig. 5). Upon addition of 10 equiv Cu^{2+} for 30 min, significant fluorescence changes could be clearly observed in cells pre-incubated with **FZU-06,001**. Flow cytometry was also used to detect the intracellular fluorescence changes. With 488

nm laser excitation, the fluorescence of **FZU-06,001** could detect through either 530 or 585 nm bandpass filters. The fluorescent intensity of cells detected through 530 nm was stronger than that detected through 585 nm. Fig. 6 shows the flow cytometry analysis of Hela and HepG2 cells incubated with **FZU-06,001** in the presence or absence of Cu^{2+} detecting through 530 nm bandpass filters. The mean fluorescent intensities of Hela and HepG2 cells pre-incubated with **FZU-06,001** significantly decreased upon addition of Cu^{2+}. The above results demonstrated that **FZU-06,001** could reveal the variation of the Cu^{2+} in biological systems.

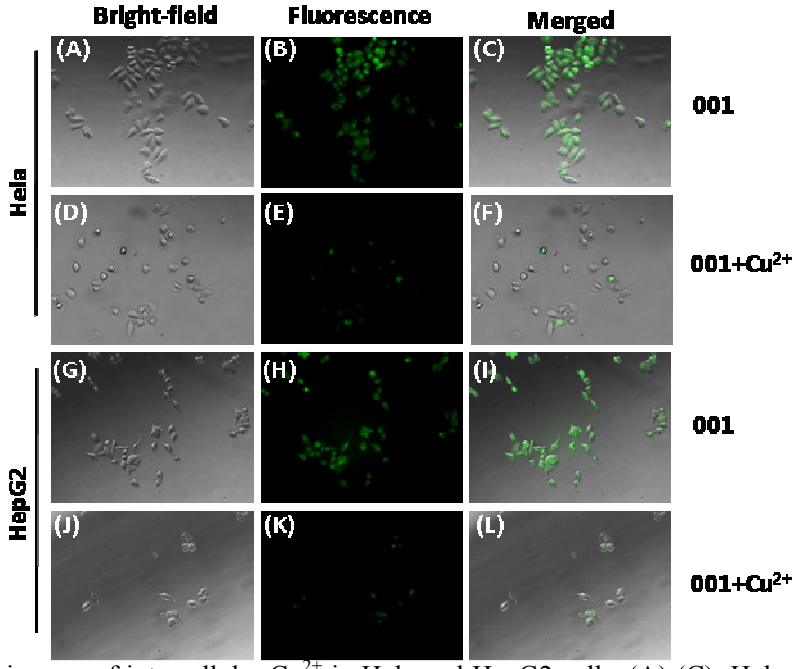

Fig. 5 Fluorescence images of intracellular Cu^{2+} in Hela and HepG2 cells. (A)-(C): Hela cells incubated with **FZU-06,001** for 2 h. (D)-(F): **FZU-06,001** stained Hela cells were exposed to 10 equiv of Cu^{2+} for 30 min. (G)-(I): HepG2 cells incubated with **FZU-06,001** for 2 h. (J)-(L): **FZU-06,001** stained HepG2 cells were exposed to 10 equiv of Cu^{2+} for 30 min.

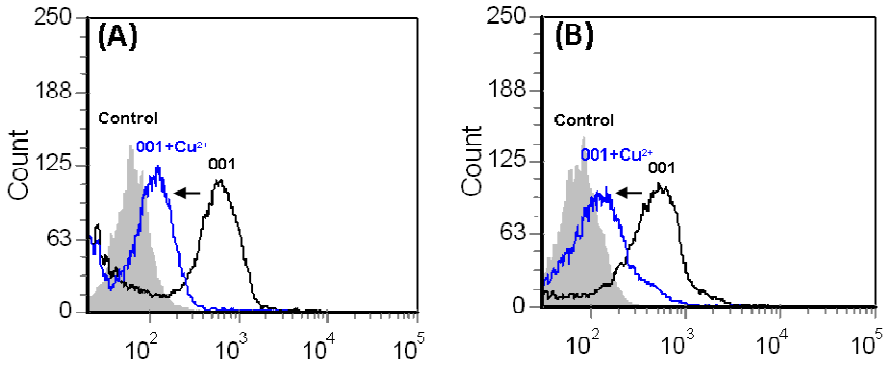

Fig. 6 FACSCalibur flow cytometry analyzed the mean fluorescent intensity of Hela cells and HepG2 cells incubated with 10 μM **FZU-06,001** for 2 h at 37 °C with or without addition of 10 equiv of Cu^{2+} for further incubation for 0.5 h. Untreated cells were used as negative control. (A) FCM pictures of Hela cells incubated with **FZU-06,001**. (B) FCM pictures of HepG2 cells incubated with **FZU-06,001**.

3.7 Chelation efficacy

MTT assay was employed to investigate the chelation efficacy of Cu^{2+} by **FZU-06,001**. The cell viability significantly decreased with increasing Cu^{2+} concentration (Fig. 7). The cell viability of Hela and HepG2 cells obviously increased upon addition of **FZU-06,001**. The cell viability increased from 48.5% to 75.6% after adding **FZU-06,001** to cells treated with 20 μM Cu^{2+}, indicating **FZU-06,001** having ability to chelate Cu^{2+} to reduce the toxic effect of Cu^{2+}.

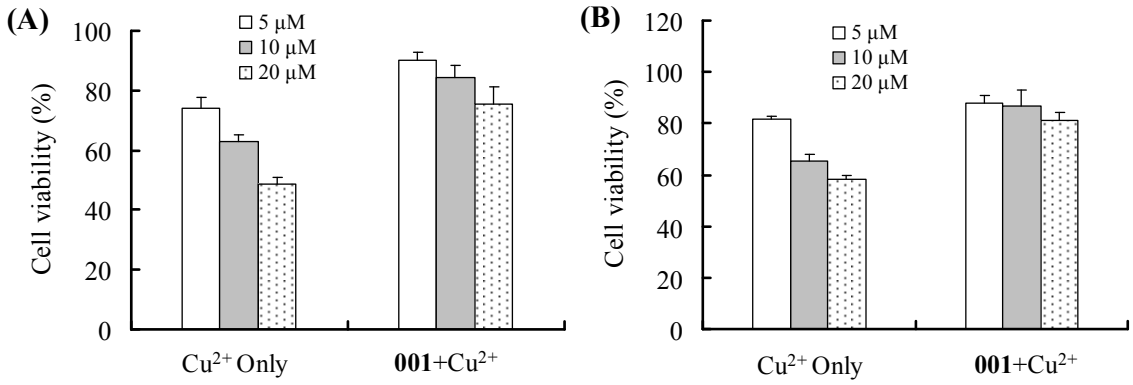

Fig. 7 Chelation efficacy of **FZU-06,001**. Hela (A) or HepG2 (B) cells were incubated with 5, 10, or 20 μM Cu^{2+} in the presence or absence of **FZU-06,001** at the same concentration for 24 h at 37 °C. Then cell viability was evaluated by MTT assay. Each data point represents the mean ± SD of six replicates.

4. Discussion

Copper as an essential element is needed for normal physiological function of human body.[21] It plays important roles in nerve function, bone growth, the formation of connective tissue, and hormone secretion. The disorder of copper metabolism in biological systems may lead to various diseases including Menkes disease, Wilson's disease, and Alzheimer's disease.[22] Additionally, the redox-active property of this metal may have toxic effects on cells due to the generation of harmful reactive oxygen species.[23] Therefore, it is very important to develop effective methods for monitoring and regulating Cu^{2+} in biological systems.

In this work, a novel Cu^{2+}-selective fluorescence sensor **FZU-06,001** was designed and synthesized for bio-detection and chelation. The moiety of quinoline was utilized to construct the coumarin derivative as a novel fluorescence sensor for accumulating evidence demonstracted that the quinoline scaffold as an important structural unit widely presents in natural and synthetic analogues with exciting biological activities.[24] We envision that the Cu^{2+} ion binds coumarin lactone, amide, and the quinoline N, which is shown in Scheme 2. In contrast, **FZU-06,002** without quinoline N had no affinity toward Cu^{2+}. As expected, obvious red shift of the absorption maximum and fluorescence quenching were observed for **FZU-06,001** upon addition of Cu^{2+} in contrast to other metal ions, while **FZU-06,002** with naphthalene moiety did not exhibited this change further indicating that 8-aminoquinoline as an very common structural fragment for traditional drug discovery is critical for Cu^{2+} chelation. **FZU-06,001** was further titrated with different concentrations of Cu^{2+} by measuring the absorbance and fluorescence emission spectra. To our delight, we found that **FZU-06,001** could sense the Cu^{2+} in a very low concentration with the detection limit as low as 0.1 μM. It was reported that heavy metal ions tend to quench the luminescence through electron- and /or energy-transfer processes.[25] Jung *et*

al. also got an insight into the quenching mechanism of a coumarin-based fluorescence probe bearing the 2-picolyl unit in the presence of Cu^{2+}, suggesting that the quenching occuring by the excitation energy transfer from the ligand to the metal d-orbital and/or ligand to metal charge transfer.[6] The fluorescence quenching pathway between **FZU-06,001** and Cu^{2+} might be similar to the aforementioned.

We further investigated the potential application of **FZU-06,001** for biological Cu^{2+} detection, the sensing ability was tested in living cells. The sensing experiment was performed under the safe concentration of **FZU-06,001** to avoid cell injury. Fluorescent imaging is one of the most direct methods to observe the sensitivity of the fluorescent chemosensor. The images clearly indicated that **FZU-06,001** could enter cells and sense the intracellular Cu^{2+} changes. The investigation of the subcellular localization of **FZU-06,001** revealed that this theranostic agent is an interesting dye for lysosomes and nuclear, indicating that it can reduce the toxic effect of Cu^{2+} in the whole cell. Flow cytometry was also used to detect the intracellular fluorescent intensity of **FZU-06,001** with addition of Cu^{2+}. The results also demonstrated that **FZU-06,001** could interact with Cu^{2+} inside the cells and the fluorescent of **FZU-06,001** could be quenched by the intracellular Cu^{2+}.

Toxic metals such as lead, copper, arsenic, aluminum, and mercury represent a significant health concern. Several studies reported about the chelation of toxic metals to reduce toxicity to living cells.[26-28] Some compounds which could silence the redox-active free Cu^{2+} ions and their binding to the protein exert the protective role in AD and other neurodegenerative disorders.[22] In the MTT study, we found that **FZU-06,001** could reduce the toxic effect of Cu^{2+} to cultured cells, indicating **FZU-06,001** could chelate Cu^{2+} inside the cells and silence the redox-active free

Cu^{2+} ions. These results demonstrated that **FZU-06,001** could be used for either detection or chelation of Cu^{2+} in cultured cells.

5. Conclusions

In conclusion, we designed and synthesized a novel fluorescence sensor (**FZU-06,001**) for detecting Cu^{2+} with high sensitivity and selectivity. The sensor showed a large red-shift in UV-vis spectra and obvious decline of fluorescent intensity in fluorescence emission spectra with Cu^{2+} over other metal ions. **FZU-06,001** did not exhibited obvious cytotoxicity further indicating that this novel sensor can be used for fluorescent imaging in long time incubation. The bio-imaging studies and flow cytometric analysis revealed that **FZU-06,001** was cell-permeable and could be used for detection of the changes of intracellular Cu^{2+}, suggesting the suitability of **FZU-06,001** for biological application. In addition, **FZU-06,001** had ability to chelate excess Cu^{2+} in cultured cells to modulate the biological functions of Cu^{2+}. In a sense of membrane permeability, biocompatibility, selectivity in detection of Cu^{2+}, and chelation of excess Cu^{2+} in living cells, **FZU-06,001** could be one of the promising fluorescent sensors combining the abilities of either detection or modulation of the biological function of Cu^{2+} in biological conditions.

Acknowledgment

This work was supported by the National Natural Science Foundation of China (Nos. 81402781 and 81571802), the Scientific Research Foundation for the Returned Overseas Chinese Scholars, and Technology Development Foundation of Fuzhou University (Project Numbers 2013-XQ-8, 2013-XQ-9, 2014-XY-7, and 2014-XY-8).

References

1. P. Delangle and E. Mintz, *Dalton Trans.*, 2012, **41**, 6359-6370.
2. S. Nomura, S. Nozaki, T. Hamazaki, T. Takeda, E. Ninomiya, S. Kudo, E. Hayashinaka, Y. Wada, T. Hiroki, C. Fujisawa, H. Kodama, H. Shintaku and Y. Watanabe, *J. Nucl. Med.*, 2014, **55**, 845-851.
3. G. Loudianos, M. B. Lepori, E. Mameli, V. Dessi and A. Zappu, *Prilozi*, 2014, **35**, 93-98.
4. R. Gonzalez-Dominguez, T. Garcia-Barrera and J. L. Gomez-Ariza, *Biometals*, 2014, **27**, 539-549.
5. T. Finkel, M. Serrano and M. A. Blasco, *Nature*, 2007, **448**, 767-774.
6. H. S. Jung, P. S. Kwon, J. W. Lee, J. I. Kim, C. S. Hong, J. W. Kim, S. Yan, J. Y. Lee, J. H. Lee, T. Joo and J. S. Kim, *J. Am. Chem. Soc.*, 2009, **131**, 2008-2012.
7. G. Cerchiaro, T. M. Manieri and F. R. Bertuchi, *Metallomics*, 2013, **5**, 1336-1345.
8. Y. W. Lin, C. C. Huang and H. T. Chang, *Analyst*, 2011, **136**, 863-871.
9. L. Quan, T. Sun, W. Lin, X. Guan, M. Zheng, Z. Xie and X. Jing, *J. Fluoresc.*, 2014, **24**, 841-846.
10. F. J. Huo, C. X. Yin, Y. T. Yang, J. Su, J. B. Chao and D. S. Liu, *Anal. Chem.*, 2012, **84**, 2219-2223.
11. Z. Liu, C. Zhang, X. Wang, W. He and Z. Guo, *Org. Lett.*, 2012, **14**, 4378-4381.
12. M. M. Li, W. B. Zhao, T. T. Zhang, W. L. Fan, Y. Xu, Y. Xiao, J. Y. Miao and B. X. Zhao, *J. Fluoresc.*, 2013, **23**, 1263-1269.
13. Y. Cao, M. A. Skaug, O. Andersen and J. Aaseth, *J. Trace Elem. Med. Biol.*, 2014, doi: 10.1016/j.jtemb.2014.1004.1010.
14. M. S. Muthu, D. T. Leong, L. Mei and S. S. Feng, *Theranostics*, 2014, **4**, 660-677.
15. O. Diou, N. Tsapis and E. Fattal, *Expert Opin. Drug Deliv.*, 2012, **9**, 1475-1487.
16. B. Zhu, P. Yang, H. Yu, L. Yan, Q. Wei and B. Du, *Nanotechnology*, 2013, **24**, 495502.
17. P. Yang, B. Zhu, J. Zhao, H. Yu, Q. Wei and B. Du, *J. Nanosci. Nanotechnol.*, 2014, **14**, 5426-5429.
18. K. Suzuki, A. Kobayashi, S. Kaneko, K. Takehira, T. Yoshihara, H. Ishida, Y. Shiina, S. Oishi and S. Tobita, *Phys. Chem. Chem. Phys.*, 2009, **11**, 9850-9860.
19. Y. Ma, W. Luo, P. J. Quinn, Z. Liu and R. C. Hider, *J. Med. Chem.*, 2004, **47**, 6349-6362.
20. H. N. Xu, H. J. Chen, B. Y. Zheng, Y. Q. Zheng, M. R. Ke and J. D. Huang, *Ultrason. Sonochem.*, 2015, **22**, 125-131.
21. Y. Ogra, *Nihon Eiseigaku Zasshi*, 2014, **69**, 136-145.
22. G. Meloni, P. Faller and M. Vasak, *J. Biol. Chem.*, 2007, **282**, 16068-16078.
23. A. Pal, J. Jayamani and R. Prasad, *Neurotoxicology*, 2014, **44**, 58-60.
24. M. Orhan Puskullu, B. Tekiner and S. Suzen, *Mini Rev. Med. Chem.*, 2013, **13**, 365-372.
25. B. B. Campos, M. Algarra, B. Alonso, C. M. Casado and J. C. Esteves da Silva, *Analyst*, 2009, **134**, 2447-2452.
26. S. J. Flora, G. Saxena and A. Mehta, *J. Pharmacol. Exp. Ther.*, 2007, **322**, 108-116.
27. V. Pachauri, G. Saxena, A. Mehta, D. Mishra and S. J. Flora, *Toxicol. Appl. Pharmacol.* , 2009, **240**, 255-264.
28. P. Hantson, V. Haufroid, J. P. Buchet and P. Mahieu, *J. Toxicol. Clin. Toxicol.*, 2003, **41**, 1-6.